



# Study on the Residual Load-Bearing Capacity of CFRP-Reinforced CFST Columns After Impact

Yaxiong He<sup>1,\*</sup>, Feng Fu<sup>2</sup>

<sup>1</sup>School of Civil Engineering, Guilin University of Technology, China, Guangxi, Guilin 541004  
China

<sup>2</sup>College of Civil Engineering, City University of London, United Kingdom, London EC1V  
0HB

\*Corresponding author's e-mail: 2120220774@glut.edu.cn

**Abstract.** Based on the simulation technology of LS-DYNA software, this study conducted comprehensive and detailed finite element simulations of concrete-filled steel tube (CFST) columns strengthened with carbon fiber-reinforced polymer (CFRP) wrapping under lateral impact loading. After validating the reliability of the simulation results by comparing them with experimental data from existing literature, this research further expanded the scope of parametric analysis. The study thoroughly investigated the influence of three key factors—CFRP ply orientation, number of reinforcement layers, and reinforcement range—on the residual compressive bearing capacity of CFST columns after lateral impact. Through a series of analyses, the following significant conclusions were drawn: (1) CFRP reinforcement significantly enhances the impact resistance of CFST columns under lateral impact loading, while effectively improving their residual compressive bearing capacity. (2) The CFRP ply angle has a notable influence on the reinforcement effect, with the compressive bearing capacity reaching its maximum when the CFRP ply angle is 0° (transverse direction), whereas it is relatively lower when the ply angle is 90° (longitudinal direction). (3) Increasing the number of CFRP layers and the reinforcement range improves the compressive bearing capacity of CFST columns, and when the reinforcement range extends to 2/3 of the clear span, the enhancement in compressive bearing capacity becomes particularly significant.

**Keywords:** CFRP; Concrete-Filled Steel Tubular Columns; Low-Speed Impact; Finite Element; LS-DYNA

## 1 Introduction

In recent years, both Chinese and international scholars have investigated the residual bearing capacity of various types of concrete-filled steel tube (CFST) columns under impact loading. Fu Chao jiang, Wang Zhong hua<sup>[1-3]</sup> designed seven CFST columns and conducted drop-hammer impact and axial compression tests to study the influence of axial compression ratio, wall thickness, and impact energy on their performance.

Gao S et al. [4] proposed a simplified formula for calculating the number of pseudo-stable impacts and the corresponding mid-span displacements of a square CFST column under repeated transverse impacts, and the results were in good agreement with the experimental and numerical results. Guo Jin long et al. [5] utilized the finite element software ABAQUS to establish a model of a circular CFST long column member, conducting dynamic response simulations of axial force-impact coupling and quasi-static vertical axial compression simulations of damaged members after impact. Zhang X et al. [6] conducted a study on the lateral impact of 48 short rectangular CFST columns, concluding that impact loading reduced the residual bearing capacity, stiffness, and ductility of the CFST columns. They also found that the impact location had a greater effect when closer to the end of the column. A comprehensive analysis of Ultra High Performance Fibre Reinforced Concrete (UHPFRC)-encased Concrete Filled Steel Tube (CFST) columns subjected to axial and eccentric compression by Du P et al [7], revealed that UHPFRC-encased CFST columns exhibited significantly enhanced strength and flexural capacity, while FRC-encased columns exhibited significant ductility. Chen et al. [8] conducted drop-hammer impact tests on CFST columns reinforced with CFRP and GFRP (glass fiber-reinforced polymer) of the same cross-sectional area but different lengths. They concluded that GFRP significantly improves the impact resistance of concrete-filled steel tubes compared to the original specimens. Gao D et al [8] conducted an experimental study on carbon fibre reinforced polymer (CFRP-CFST) constrained rectangular high-strength concrete-filled steel tubular columns under eccentric compression, and explored the effects of key parameters including eccentricity, number of transverse CFRP layers, length-to-slender ratio, radius of fillet, CFRP wrapping scheme, and direction of CFRP on CFST columns. However, most of these studies are limited to the performance of CFST columns during impact, with relatively little discussion on the residual bearing capacity after impact. Therefore, based on existing research, this paper will focus on analyzing the failure mechanism of the residual bearing capacity of CFRP-strengthened CFST columns after impact. The relevant experiments of Chen [8] will be simulated using the ANSYS/LS-DYNA finite element software to explore the influence of CFRP reinforcement methods on the residual bearing capacity and reveal its mechanism.

## 2 Finite Element Modelling

### 2.1 Experimental

Chen et al. [8] conducted an experimental study on eleven CFST specimens with identical cross-sectional areas but varying lengths to examine their structural behavior under impact loading. The study included eight CFRP-reinforced columns, two GFRP-reinforced columns, and one unreinforced CFST column as a control. Time-history curves of impact force, acceleration, deflection, and strain were recorded to analyze the dynamic response. All specimens had a 107 mm concrete core diameter, 3.5 mm steel tube thickness, and spans ranging from 1400 to 1700 mm (Figure 1), with impact loads applied at mid-span.

The CFST cores were reinforced with CFRP or GFRP in single or double layers using transverse or longitudinal wrapping methods, with each layer being 0.17 mm thick. This study selected four specimens for finite element simulation, focusing on key variables such as length, CFRP layer count, and wrapping methods (transverse or longitudinal). Detailed parameters, including material properties and geometric dimensions, are provided in Table 1. This approach enabled a comparison between experimental and numerical results, offering insights into the impact resistance and load-bearing capacity of CFRP-reinforced CFST columns.

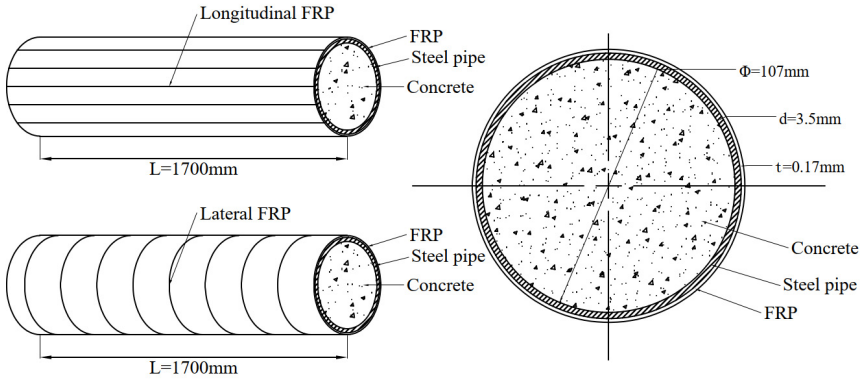


**Fig. 1.** Specimen Schematic Diagram

**Table 1.** Details of specimens

Specimen	Length (mm)	CFRP layers	FRP wrapping direction
LCL1	1700	1	Longitudinal
LCL2	1700	2	Longitudinal
SCL1	1400	1	Longitudinal
LWW	1700	-	-

Note: The first characters L = long specimen, S = short specimen. The second characters (C and W): C = CFRP, W = no FRP. The third characters. L = longitudinal FRP. The number 1 or 2 indicates a specimen with one- or two-layer FRP. For example, LCL1 = concrete-filled steel tube (1,700 mm) reinforced with one-layer longitudinal CFRP; One-layer CFRP = 0.17 mm; one-layer.

As illustrated in Figure 2, impact loading was performed using a drop-weight impact testing machine. A hemispherical drop-weight, with a mass of 80 kg and a diameter of 150 mm, was released from a height of 1.5 m to impact the mid-span of the CFST column. The impact force was measured using a force transducer, which was secured to the specimen via a clamping mechanism. A steel plate was positioned between the drop-weight and the force transducer to safeguard the latter.

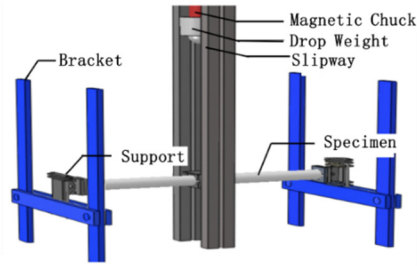


Fig. 2. Drop Weight Impact Testing Apparatus [8]

## 2.2 Model Establishment

To validate the reliability and accuracy of the residual bearing capacity analysis of CFRP-confined concrete-filled steel tube (CFST) columns, this study employs LS-DYNA software to simulate the transverse impact on CFRP-confined CFST columns [10]. Utilizing LS-Pre-Post for pre- and post-processing, the numerical model is validated through experimental comparisons. Subsequently, a residual bearing capacity analysis is conducted. This paper presents numerical simulations of the LCL1, LCL2, SCL1, and LWW specimens from the experimental program. Three-dimensional finite element model of a CFRP-strengthened CFST column was established using ANSYS-LS-DYNA. The impactor, simplified as a hemispherical shape, was assigned a specific density to simulate its impact mass. A 2 mm gap was set between the impactor and the specimen, and the impactor was assigned an initial impact velocity. Automatic surface-to-surface contact was defined between the impactor and the column, with a friction coefficient of 0.3, while other parameters were set to default values. The concrete was modeled using the \*MAT\_CSCM\_CONCRETE material model, with the IRATE keyword, which controls strain rate effects, set to 1. The remaining parameters were determined based on the compressive strength ( $f_c$ ) and aggregate size ( $A_g$ ) as described in the CSCM user manual. The steel material was modeled using the \*MAT\_PLASTIC\_KINEMATIC model, and the CFRP material model utilized the \*MAT\_ENHANCED\_COMPOSITE\_DAMAGE option. A detailed illustration of the finite element model is presented in Figure 3.

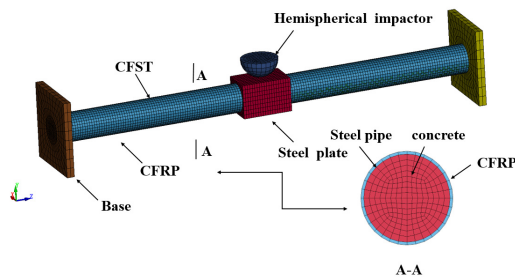


Fig. 3. Finite Element Model

### 3 Finite Element Model Validation

#### 3.1 Impact Force Comparison

As shown in Figure 4, analyzing the curves, it can be seen that the overall trend of the test results of the impact force of each specimen is consistent with the simulation results, and the maximum error between the test and the simulation is not more than 14%, which indicates that the time-course curve of the impact force of the two basically coincides with each other, and the finite element model can predict the time-course curve of the impact force of the specimen better.

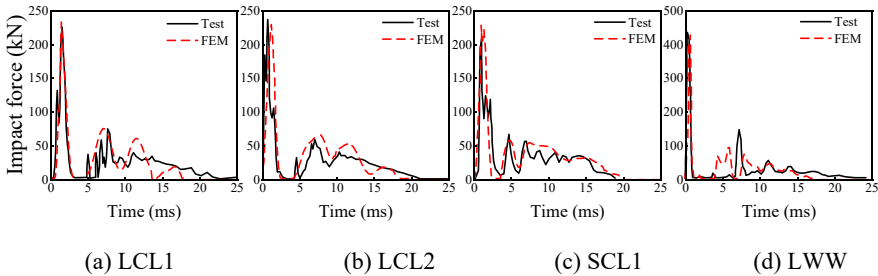


Fig. 4. Comparison of Impact Force-Time Curves

#### 3.2 Comparison of Mid-Span Deflection

The change of mid-span displacement is shown in Fig. 5. From the curve in the figure, it can be seen that the simulation results and the change trend of the displacement curve keep the same change characteristics, and the error of its peak size is also within 5%, which shows that the finite element model can predict the mid-span displacement of the test specimen better.

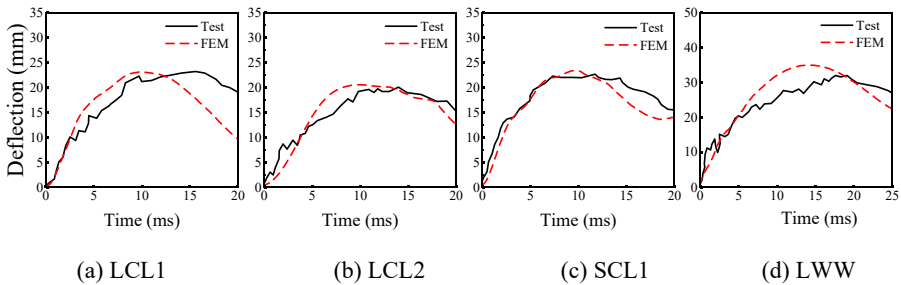


Fig. 5. Mid-span Deflection Curve

## 4 Residual Load-Bearing Capacity Analysis

For CFRP-reinforced CFST columns subjected to impact loading, their residual load-bearing capacity is influenced by a variety of factors. This study focuses on exploring the effects of CFRP ply orientation, CFRP wrapping length, and the number of CFRP wrapping layers on the post-impact residual load-bearing capacity of CFST columns. Detailed parameter variables, including specific dimensions, material properties, and loading conditions, are comprehensively listed in Table 2. Furthermore, to better understand the structural behavior under impact, the axial load–lateral displacement curves for each reinforced column after impact are systematically plotted and analyzed in Fig. 6, providing insights into the deformation and failure mechanisms.

**Table 2.** Details of specimens

Specimen	layers	Angle	length
A0	1	0°(Transverse)	L
A45	1	45°	L
A90	1	90°(Longitudinal)	L
F1	1	0°	L
F2	2	0°	L
F3	3	0°	L
L560	1	0°	0.33L
L1120	1	0°	0.66L
L1680	1	0°	0.99L
LWW	–	–	–

Note: The letters A, F, L represent different angles, numbers of layers, and lengths of CFRP, respectively. L is the clear span of the CFST column. LWW refers to the impact-unreinforced CFST column.

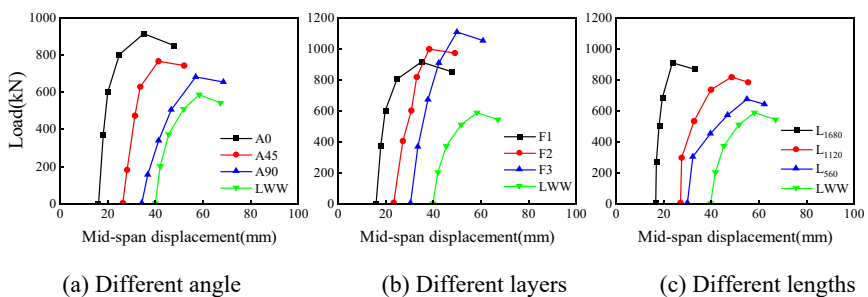


**Fig. 6.** Axial load-transverse mid-span displacement curve

As illustrated in Fig. 6 and Table 2, CFRP-reinforced CFST columns significantly influence the impact resistance and residual load-bearing capacity of CFST columns. Under various CFRP reinforcement conditions, the compressive load-bearing capacity of reinforced columns after impact increases by 15.07% to 89.55% compared to unreinforced columns (LWW). This indicates that the structural design of CFST columns

should consider incorporating different CFRP reinforcement configurations to effectively enhance their impact resistance and post-damage residual load-bearing capacity.

### 4.1 CFRP Layup Orientation

As shown in Fig. 7-a, CFRP-reinforced columns exhibit a 16.27% to 56.16% increase in compressive load-bearing capacity compared to unreinforced columns. However, as the CFRP ply angle increases, the load-bearing capacity decreases, reaching its lowest at 90°, which is 25.55% lower than at 0° (hoop direction). Fig. 7-c indicates that with increasing axial load, the lateral deflection curve of the specimen gradually assumes a sinusoidal shape. Lateral deformation develops slowly when the axial load is between 0 and 0.8 Fu (Fu being the ultimate load-bearing capacity), but accelerates significantly beyond 0.8 Fu due to intensified damage. These results demonstrate that for impact-damaged CFST columns, lateral deformation progresses slowly at axial loads ≤ 0.8 Fu but rapidly beyond this threshold. CFRP reinforcement enhances the residual load-bearing capacity to varying degrees within the range of 0° ≤ θ ≤ 90°, with the maximum capacity achieved at 0° (hoop direction) and the minimum at 90° (longitudinal direction). Therefore, transverse CFRP reinforcement is the most effective method for improving the post-impact residual load-bearing capacity of CFST columns.

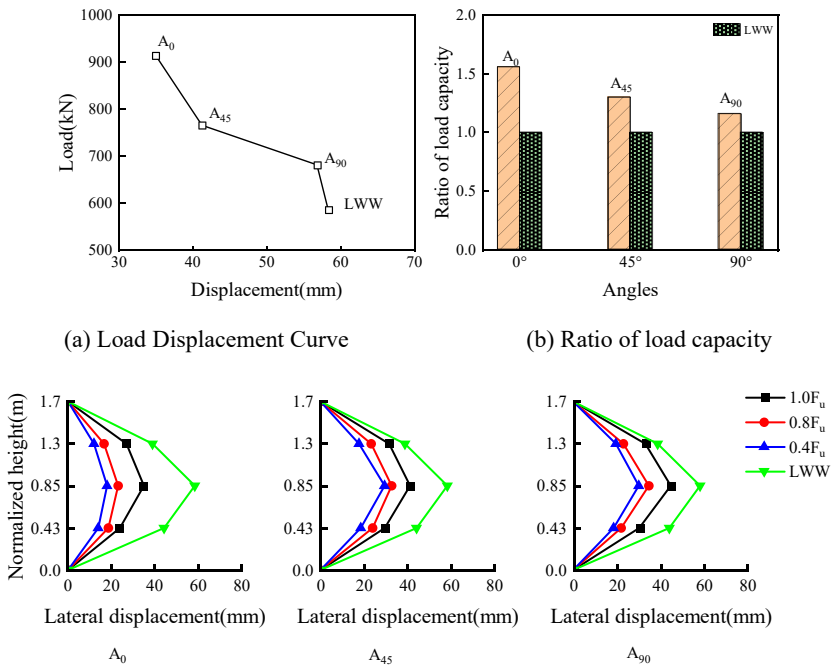


Fig. 7. Effect of Angles

## 4.2 Number of CFRP Strengthening Layers

From Fig. 8-a, the transverse displacement of the impact-reinforced column increases with more CFRP layers, showing that additional layers enhance compressive load-bearing performance. Fig. 8-b indicates the load-bearing capacity ratio of reinforced to unreinforced columns rises from 1.6 to 1.9, demonstrating CFRP's effective circumferential confinement. Similarly, when axial load  $\leq 0.8 F_u$ , transverse deformation develops slowly, but accelerates beyond  $0.8 F_u$  due to damage. Thus, increasing CFRP layers appropriately improves compressive load-bearing capacity.

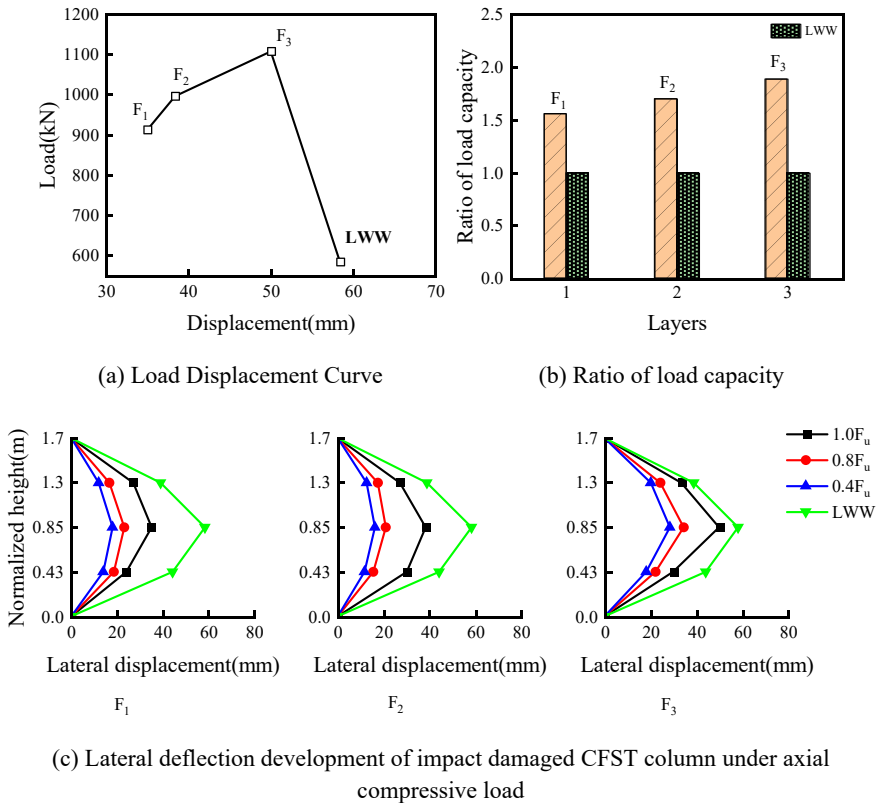


Fig. 8. Effect of layers

## 4.3 Length of CFRP Strengthening

The range of CFRP wraps extends uniformly from the impact point of the specimen to both ends with specific dimensions of 560 mm (0.33 L), 1120 mm (0.66 L), and 1680 mm (0.99 L) (L is the net span length of CFRP-reinforced CFST columns). The maximum compressive bearing capacity and maximum transverse displacement of the reinforced and unreinforced columns with different CFRP fiber lengths after impact, as well as the ratio of the compressive bearing capacity of the reinforced columns to that

of the unreinforced columns under the same impact, and the overall transverse deflection curves of the specimens at the level of axial load are shown in Fig. 9.

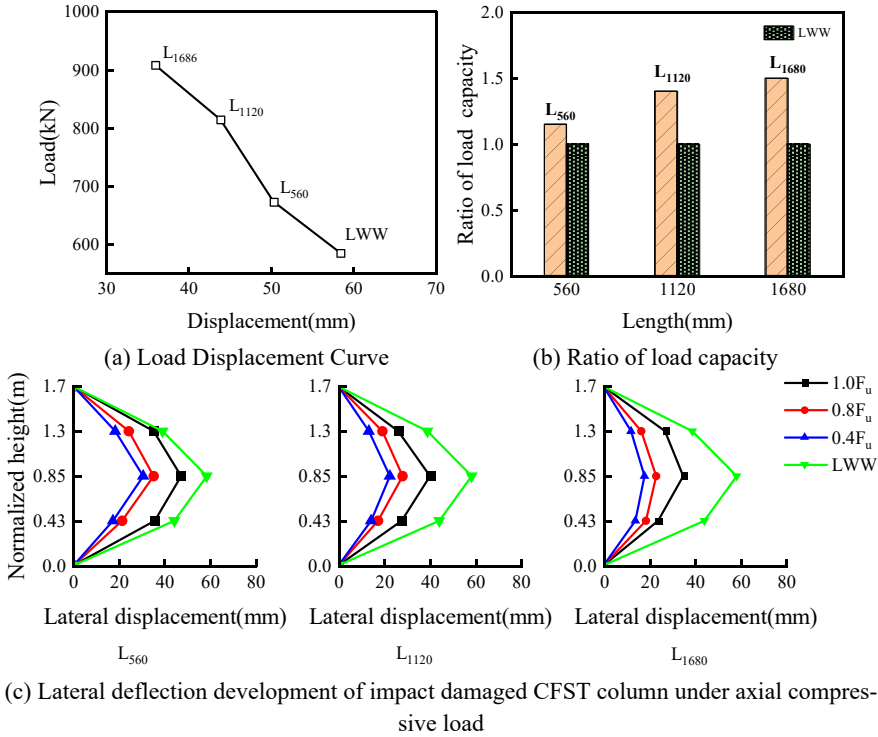


Fig. 9. Effect of length

Fig. 9 clearly demonstrates that increasing the CFRP wrapping range significantly enhances the compressive load-bearing capacity of CFST columns. As illustrated in Fig. 9-b, the capacity ratio exhibits a progressive increase with the wrapping length: the ratios are 1.1 for L<sub>560</sub>, 1.4 for L<sub>1120</sub>, and 1.5 for L<sub>1680</sub>, corresponding to improvements of 27.27% and 7.14% over the L<sub>560</sub> specimen, respectively. This trend highlights that expanding the CFRP wrapping range from 1/3 of the clear span (560 mm) to 2/3 of the clear span (1120 mm) results in a substantial enhancement in the compressive capacity of CFST columns. These findings underscore that a CFRP reinforcement range within 1/3 to 2/3 of the clear span is particularly effective in improving structural performance. For optimal design outcomes, it is recommended to adopt a CFRP wrapping range of 2/3 of the clear span, while other sections of the column can be reinforced with more ductile and cost-effective FRP materials to achieve a balance between performance and economic efficiency.

## 5 Conclusions

(1) CFRP reinforcement significantly improves the impact resistance and residual bearing capacity of CFST columns. After impact loading, the compressive bearing capacity of the reinforced columns increased by 56.16% to 88.35% compared with the unreinforced columns.

(2) CFRP reinforcement significantly enhanced the compressive capacity of columns, with residual capacity decreasing as the lay-up angle increased, peaking at  $0^\circ$  (circumferential direction). Lateral deformation progressed slowly at axial loads  $\leq 0.8 F_u$  ( $F_u$  being the maximum capacity), but accelerated significantly beyond this threshold.

(3) Increasing the CFRP wrapping range enhances the compressive load-bearing capacity, particularly when the wrapping range extends from  $1/3$  to  $2/3$  of the clear span, where the improvement is most significant. Therefore, a reasonable CFRP wrapping range (e.g.,  $2/3$  of the clear span) should be selected in the design of reinforcement schemes.

The study showed that CFRP reinforcement significantly improved the residual load carrying capacity of CFST columns, but there were some shortcomings in the study, such as the lack of theoretical analysis of the damage mechanism of CFRP-reinforced CFST columns or the damage mechanism of CFR-reinforced columns under more complicated working conditions. Therefore, future research should focus on the theoretical analysis of CFRP-reinforced CFST columns and the possible damage under more complicated working conditions.

## Reference

1. FU Chao jiang, ZHANG Ting, CHEN Hua yan, et al. Experimental study on axial compressive mechanical properties of steel pipe concrete columns after impact. *Building Structure*, 2024, 54 (16): 25-31+7. DOI: 10.19701/j.jzjg.LS230047.
2. FU Chao jiang, WANG Zhong hua, WANG Ke. Study on residual bearing capacity and damage of circular steel pipe concrete columns under lateral impact. *Building Science*, 2021, 37 (05): 11-20+27. DOI: 10.13614/j.cnki.11-1962/tu.2021.05.002.
3. FU Chao jiang, GAO Ying, CHEN Hua yan, et al. Study on residual axial compressive capacity of steel-tube concrete columns after lateral impact. *Advances in Architectural Steel Construction*, 2024, 26 (04): 57-69. DOI: 10.13969/j.cnki.cn31-1893.2024.04.007
4. Gao S, Yang J, Kang B S, et al. Experimental and numerical studies on deformation performance of square concrete-filled steel tubular columns under repeated lateral impacts. *Engineering Structures*, 2024, 308 117909-.
5. GUO Jin long, PAN Shuang, FU Shiqi. Study on the vertical residual load carrying capacity of circular hollow sandwich steel-tube concrete long columns after lateral impact action. *Engineering Mechanics*, 1-13 [2025-03-06]. <http://kns.cnki.net/kcms/detail/11.2595.O3.20230703.1855.008.html>.
6. Zhang X, Chen Y, Wan J, et al. Tests on residual ultimate bearing capacity of square CFST columns after impact. *Journal of Constructional Steel Research*, 2018.

7. Du P, Ma X Y, Tan H K. Experimental study of ultra-high-performance fibre-reinforced concrete (UHPFRC)-encased CFST short columns under axial and eccentric compression. *Engineering Structures*, 2024, 316 118452-118452.
8. Chen C, Zhao Y, Li J. Experimental Investigation on the Impact Performance of Concrete-Filled FRP Steel Tubes. *Journal of Engineering Mechanics*, 2015, 141 (2): 04014112 - 04014112.
9. Gao D, Du Y, Chen Z, et al. Behavior of CFRP confined rectangular high-strength concrete-filled steel tubular columns under eccentric compression. *Engineering Structures*, 2024, 321 119006-119006.
10. Xian hui L, Yao Y, Tie ying L, et al. Analytical Study on Reinforced Concrete Columns and Composite Columns under Lateral Impact. *Coatings*, 2023, 13 (1): 152-152.

**Open Access** This chapter is licensed under the terms of the Creative Commons Attribution-NonCommercial 4.0 International License (<http://creativecommons.org/licenses/by-nc/4.0/>), which permits any noncommercial use, sharing, adaptation, distribution and reproduction in any medium or format, as long as you give appropriate credit to the original author(s) and the source, provide a link to the Creative Commons license and indicate if changes were made.

The images or other third party material in this chapter are included in the chapter's Creative Commons license, unless indicated otherwise in a credit line to the material. If material is not included in the chapter's Creative Commons license and your intended use is not permitted by statutory regulation or exceeds the permitted use, you will need to obtain permission directly from the copyright holder.

